Journal of Medicinal Chemistry

Article

pubs.acs.org/jmc

A New Class of Highly Potent and Selective Endomorphin-1 Analogues Containing α-Methylene-β-aminopropanoic Acids (Map)

Yuan Wang,[§] Yanhong Xing,[§] Xin Liu,[§] Hong Ji, Ming Kai, Zongyao Chen, Jing Yu, Depeng Zhao, Hui Ren, and Rui Wang*

Key Laboratory of Preclinical Study for New Drugs of Gansu Province, School of Basic Medical Sciences, Institute of Biochemistry and Molecular Biology, School of Life Sciences, Lanzhou University, Lanzhou, 730000, P. R. China

Supporting Information

ABSTRACT: A new class of endomorphin-1 (EM-1) analogues were synthesized by introduction of novel unnatural α-methylene-β-amino acids (Map) at position 3 or/and position 4. Their binding and functional activity, metabolic stability, and antinociceptive activity were determined and compared. Most of these analogues showed high affinities for the μ-opioid receptor and an increased stability in mouse brain homogenates compared with EM-1. Examination of cAMP accumulation and ERK1/2 phosphorylation in HEK293 cells confirmed the agonist properties of these analogues. Among these new analogues, H-Tyr-Pro-Trp-(2-furyl)Map-NH_2 (analogue **12**) exhibited the highest binding potency (K_i^{μ} = 0.221 nM) and efficacy (EC_{50} = 0.0334 nM, E_{max} = 97.14%). This analogue also displayed enhanced antinociceptive activity in vivo in comparison to EM-1. Molecular modeling approaches were then carried out to demonstrate the interaction pattern of these analogues with the opioid receptors. We found that, compared to EM-1, the incorporation of our synthesized Map at position 4 would bring the analogue to a closer binding mode with the μ-opioid receptor.

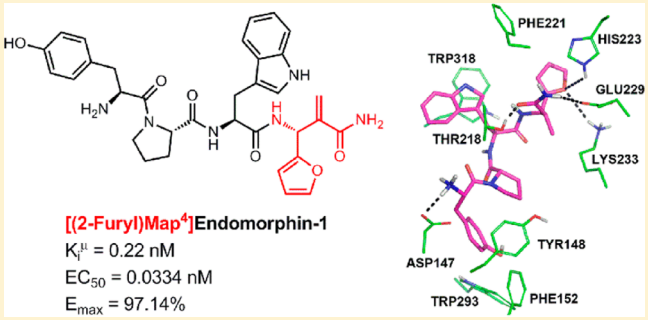

INTRODUCTION

The opioid system is one of the most studied pain relieving systems, and it consists of three subtype receptors: the μ opioid receptor (MOR), the δ opioid receptor (DOR), and the κ opioid receptor (KOR).[1] Opioid peptides serve as endogenous neurotransmitters and exert their pharmacological functions through these receptors.[2] Opioid peptides have been studied extensively since their discovery, and many efforts have been dedicated to the determination of their intrinsic nature.[3] In 1997, the MOR endogenous tetrapeptides, endomorphin-1 (EM-1, H-Tyr-Pro-Trp-Phe-NH_2) and endomorphin-2 (EM-2, H-Tyr-Pro-Phe-Phe-NH_2), were isolated from the bovine brain and the human cortex. These peptides exhibited the highest affinity for the MOR and a high MOR over DOR selectivity.[4,5] Furthermore, EMs are thought to inhibit pain without some of the undesirable side effects of morphine. Particularly, the rewarding effect of EMs can be separated from analgesia,[6] and they are less prone to induce respiratory depression and cardiovascular effects at effective antinociceptive doses.[7] For these reasons, EMs have attracted much attention from the peptide chemist/pharmacologist teams and have been considered as useful pharmacological tools with a tremendous potential in pain alleviation.[8,9] However, EMs still suffer from serious limitations including lack of oral activity, short duration of action, poor metabolic stability, and relative inability to cross the blood−brain barrier (BBB) and access the central nervous system (CNS).[10] Therefore, it is essential to enhance their bioavailability in order to facilitate therapeutic use.

For the past several years, hundreds of EM based compounds have been designed and synthesized to explore the importance of specific residues and to gain insight into the structural requirements for bioavailability.[9,11] According to the "message−address" concept, EMs can be divided into two components: the biologically important N-terminal Tyr-Pro-Trp/Phe fragment (message sequence) and the remaining C-terminal fragment (address sequence).[12,13] In the message sequence, Tyr^1 is widely considered to be the most conserved residue and essential to the opioid activity of EMs, the aromatic groups at positions 1 and 3 of endomorphins are required for MOR recognition,[14] and Pro^2 is thought to be a spacer residue that joins the two pharmacophore residues Tyr^1 and Trp^3/Phe^3. On the other hand, the address sequence (Phe^4-NH_2) is considered to influence mainly binding affinity and selectivity.[15,16] The main synthetic strategies in the chemical modification of EMs involve the insertion of unnatural amino acids, alteration of the peptide backbone, modification of the pharmacophore groups, and introduction of side chain/backbone conformational constraints.[17−20]

β-Amino acids are an interesting class of physiologically active compounds for medicinal chemists.[21−23] Endomorphins

Received: May 11, 2012
Published: June 22, 2012

dx.doi.org/10.1021/jm300664y | J. Med. Chem. 2012, 55, 6224−6236

Scheme 1. Synthesis of Unnatural β-Amino Acids Map[a]

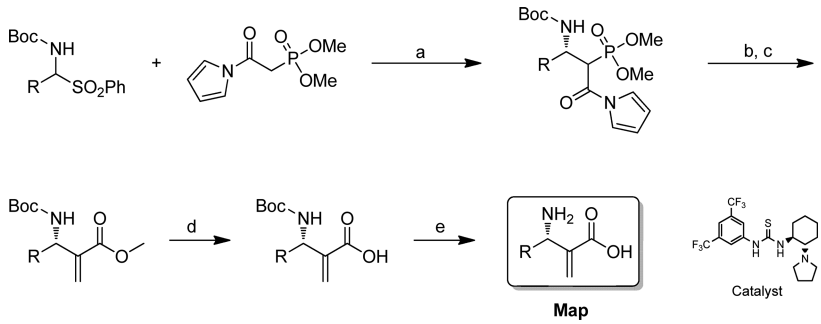

[a]Reagents and conditions: (a) catalyst 20% mol, K_2CO_3 (1.5 M, 1.2 equiv), toluene, 0 °C, 24 h, 83−92%; (b) NaOMe (2.2 equiv), THF, −15 °C, 30 min; (c) $(HCHO)_n$ (5 equiv), −15 °C, 8 h, 89−93%; (d) LiOH (aq, 1.5 equiv), THF, rt, 12 h, 95−98%; (e) HCl/EA (v/v = 1:4), rt., 2 h, 95−99%.

containing β-amino acids are generally more stable toward proteolysis, and in some cases replacement of the α-amino acids with the β-amino acids results in improved activity.[24−29] However, the β-amino acids improve the activity of EMs only when they were placed at position 2 as a stereochemical spacer. When they were incorporated at other positions, a great decrease of affinity was observed.[26,27] Considering the structural features of a β-amino acid, its flexible backbone structure possibly hindered the EMs from choosing an ideal space orientation.

In this paper, we introduced a series of novel unnatural β-amino acids (2-methylene-3-aminopropanoic acids (Map)) into EM-1. Unlike normal β-amino acids, Map is characterized by a methylene at the Cα position. This C═C bond generates a conformational constraint on the backbone structure and provides more rigidity to the molecule. A new methodology that had been developed by our group was employed to obtain this kind of unnatural β-amino acids.[30] The strategy was fulfilled by asymmetric addition of *N*-acylpyrrole phosphonates to *N*-*tert*-butyloxycarbonyl (*N*-Boc) imines generated in situ catalyzed by a bifunctional thiourea catalyst. Then the corresponding Mannich adducts were further transformed to aza-Morita−Baylis−Hillman (MBH) products by Horner−Wadsworth-Emmons (HWE) olefination with good to excellent enantioselectivities. Subsequently, the desired Map could be afforded by saponification of the corresponding methyl ester (Scheme 1). Importantly, compared with conventional aza-MBH reaction, which often provides *N*-Tos products in which the tosyl group was not easily deprotected, the present method could produce the required Map protected by the *N*-Boc group which could be removed under mild acidic conditions in a normal approach of polypeptide synthesis. Furthermore, the side chains of these unnatural amino acids could be replaced with many other aromatic or heteroaromatic groups to provide more Map derivatives with different pharmacophore elements (Table 1).

The Map were employed to substitute the residue at position 3 or/and position 4 in the hope of improving the bioactivity and enzyme resistance of EM-1. The opioid receptor affinity and in vitro opioid activities of these analogues were determined by radioligand binding experiments with [^{3}H]DAMGO in HEK293 cells stably expressing MOR and GPI/MVD bioassays,[31,32] respectively. Then the agonist/antagonist profiles of these analogues were assessed in cyclic AMP accumulation and ERK1/2 phosphorylation assays. Furthermore, the degradation rate of these analogues was examined in the presence of mouse brain homogenate, and their in vivo antinociceptive activities were characterized by a tail-flick test after intracerebroventricular (icv) administrations in mice. Finally, molecular modeling approaches were employed to gain more insight into the structure−activity relationship between the analogues and MOR.

Table 1. Maps Used in This Study

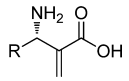

Amino Acid	R	Amino Acid	R
(Ph)Map		(Piperonyl)Map	
(4-FPh)Map		(2-Furyl)Map	
(4-ClPh)Map		(3-Furyl)Map	
(3-ClPh)Map		(1-Naphthyl)Map	
(2-ClPh)Map		(2-Naphthyl)Map	
(4-MeOPh)Map			

RESULTS

Synthesis. Endomorphins and their analogues were obtained by solution-phase methods with segment-coupling peptide synthesis strategy. Chiral 2-methylene-3-aminopropanoic acids (Map) were prepared by using the method we have published (see the Experimental Section and Supporting Information for experimental details).[30] Synthesis of all the analogues was conducted by performing an active ester reaction, and EDC and HOBt were used as coupling agents. Peptides were purified using semipreparative RP-HPLC and characterized by RP-HPLC, TLC, ESI-TOF MS, $[\alpha]^{D}_{20}$, and mp. Purities were determined to be 95−99% and characterized by analytical RP-HPLC. Table 1 outlined the Map used in this study. The detailed analytical properties of the synthetic analogues are provided in Table S1 in the Supporting Information.

Radioligand Binding and Selectivity. The affinity and selectivity of EMs and the analogues were evaluated by radioligand binding assay in whole cell preparations from HEK293 cells expressing the MOR or DOR. [^{3}H]DAMGO and [^{3}H]DPDPE were used as MOR and DOR specific radioligands, respectively. EM-1 and EM-2 were also characterized for comparison, and the affinity values were in agreement with those published previously.[4,28,33] The opioid receptor binding

dx.doi.org/10.1021/jm300664y | J. Med. Chem. 2012, 55, 6224−6236

Table 2. Opioid Receptor Binding Affinities and in Vitro Pharmacological Activity of EMs and Analogues

					IC_{50} (nM)[d]		
peptide	sequence	K_i^{μ} (nM)[a,c]	K_i^{δ} (nM)[b,c]	selectivity K_i^{δ}/K_i^{μ}	GPI	MVD	MVD/GPI[e]
1	Tyr-Pro-Trp-Phe-NH_2	2.60 ± 0.21	6080 ± 640	2338	14.1 ± 1.7	30.4 ± 2.6	2.2
2	Tyr-Pro-Phe-Phe-NH_2	3.20 ± 0.13	6420 ± 330	2006	9.33 ± 1.12	21.6 ± 3.4	2.3
3	Tyr-Pro-(Ph)Map-Phe-NH_2	103 ± 2	59290 ± 5680	576	20.9 ± 2.37	>10000	
4	Tyr-Pro-Trp-(Ph)Map-NH_2	0.535 ± 0.076	56010 ± 5180	104692	6.81 ± 0.80	7.53 ± 1.22	1.1
5	Tyr-Pro-(Ph)Map-(Ph)Map-NH_2	15.7 ± 0.4	10980 ± 1680	699	38.1 ± 1.2	166 ± 34	4.4
6	Tyr-Pro-Trp-(4-FPh)Map-NH_2	13.7 ± 0.9	17040 ± 2050	1244	31.5 ± 1.5	130 ± 14	4.1
7	Tyr-Pro-Trp-(4-ClPh)Map-NH_2	7.12 ± 1.05	10810 ± 1340	1518	15.3 ± 3.2	36.7 ± 7.0	2.4
8	Tyr-Pro-Trp-(3-ClPh)Map-NH_2	3.49 ± 0.25	5820 ± 450	1668	7.66 ± 0.51	69.4 ± 7.4	9.1
9	Tyr-Pro-Trp-(2-ClPh)Map-NH_2	5.48 ± 0.38	14930 ± 1620	2724	16.6 ± 3.7	365 ± 14	22
10	Tyr-Pro-Trp-(4-MeOPh)Map-NH_2	4.83 ± 0.91	10200 ± 1430	2112	84.2 ± 2.0	299 ± 14	3.6
11	Tyr-Pro-Trp-(piperonyl)Map-NH_2	7.73 ± 1.02	18690 ± 1330	2418	14.3 ± 1.7	432 ± 10	30
12	Tyr-Pro-Trp-(2-furyl)Map-NH_2	0.221 ± 0.014	50010 ± 2880	226290	2.92 ± 0.31	15.8 ± 0.9	5.4
13	Tyr-Pro-Trp-(3-furyl)Map-NH_2	0.274 ± 0.066	50930 ± 6710	185876	3.94 ± 0.60	10.2 ± 1.2	2.6
14	Tyr-Pro-Trp-(1-naphthyl)Map-NH_2	26.0 ± 3.5	84680 ± 10490	3264	33.9 ± 6.2	84.4 ± 6.8	2.5
15	Tyr-Pro-Trp-(2-naphthyl)Map-NH_2	27.4 ± 0.8	84850 ± 9650	3097	18.2 ± 3.8	141 ± 6	7.7

[a]Displacement of [^{3}H]DAMGO (K_d = 0.6 nM, μ-selective). [b]Displacement [^{3}H]DPDPE (K_d = 2.8 nM, δ-selective). [c]Displacement was done using whole cell preparations from transfected HEK293 cells expressing μ-opioid receptor and δ-opioid receptor, respectively. K_i values were calculated according to the Cheng–Prusoff equation: $K_i = EC_{50}/(1 + [\text{ligand}]/K_d)$, where the shown K_d values were taken from isotope saturation experiments. Data are expressed as the mean ± SEM, $n \geq 3$, each performed in triplicate. [d]Values represent the average of 10–15 measurements. [e]Potency ratio.

Table 3. Functional Activity of EMs and Analogues[a]

peptide	sequence	EC_{50} (nM)	E_{max} (%)
0	DAMGO	3.04 ± 0.32	98.14 ± 6
1	Tyr-Pro-Trp-Phe-NH_2	14.40 ± 0.62	83.13 ± 4
2	Tyr-Pro-Phe-Phe-NH_2	11.80 ± 0.23	82.75 ± 4
3	Tyr-Pro-(Ph)Map-Phe-NH_2	36.50 ± 2.45	70.78 ± 2
4	Tyr-Pro-Trp-(Ph)Map-NH_2	0.16 ± 0.09	97.94 ± 3
5	Tyr-Pro-(Ph)Map-(Ph)Map-NH_2	45.09 ± 4.01	60.26 ± 6
6	Tyr-Pro-Trp-(4-FPh)Map-NH_2	7.35 ± 1.02	81.45 ± 6
7	Tyr-Pro-Trp-(4-ClPh)Map-NH_2	12.00 ± 0.98	85.57 ± 11
8	Tyr-Pro-Trp-(3-ClPh)Map-NH_2	0.72 ± 0.08	92.53 ± 4
9	Tyr-Pro-Trp-(2-ClPh)Map-NH_2	0.84 ± 0.03	82.57 ± 4
10	Tyr-Pro-Trp-(4-MeO)Map-NH_2	10.91 ± 0.83	85.56 ± 3
11	Tyr-Pro-Trp-(Piperonyl)Map-NH_2	10.70 ± 1.09	83.90 ± 5
12	Tyr-Pro-Trp-(2-Furyl)Map-NH_2	0.0334 ± 0.0012	97.14 ± 5
13	Tyr-Pro-Trp-(3-Furyl)Map-NH_2	0.0342 ± 0.0018	98.73 ± 5
14	Tyr-Pro-Trp-(1-Naphthyl)Map-NH_2	72.30 ± 6.00	71.01 ± 4
15	Tyr-Pro-Trp-(2-Naphthyl)Map-NH_2	70.34 ± 4.67	67.46 ± 5

[a]Effects of peptides on forskolin stimulated cyclic AMP accumulation by μ-opioid receptor. HEK293 cells expressing MOR were stimulated with increasing concentrations of the indicated peptides as described in the Experimental Section. EC_{50} and E_{max} values were calculated by using the GraphPad Prism software. Data were means ± SEM, $n \geq 3$, each performed in triplicate.

properties of the analogues were summarized in Table 2. The analogue in which Trp^3 was replaced by (Ph)Map (**3**) exhibited about 39.6-fold lower μ-affinity and 9.8-fold lower δ-affinity than EM-1. However, substitution of Phe^4 with (Ph)Map gave analogue **4** with about 4.9-fold increase in μ-affinity (K_i^{μ} = 0.535 nM) and 9.2-fold decrease in δ-affinity (K_i^{δ} = 56,010 nM), thus resulting in a remarkable increase in μ-selectivity. The corresponding substitution, performed at both positions 3 and 4, led to analogue **5** which exhibited about 6-fold lower μ-affinity compared with the parent. Thus, subsequent modifications were performed mainly on the aromatic group of position 4. Substitution of the Phe^4 with (4-FPh)Map afforded analogue **6** with reduced potency in comparison with parent peptide. Analogues **7**–**11** displayed relatively high μ-affinity, with binding affinities ranging from 3.49 to 7.73 nM, and their selectivities were similar to that of EM-1. It was noteworthy to mention that **8** displayed the highest δ-affinity in all the synthesized analogues. Analogues **12** and **13** bearing a furyl ring were the two most potent peptides. Their μ-affinity increased about 10-fold (K_i^{μ} of 0.221 and 0.274 nM, respectively), and their δ-affinity decreased about 8-fold over EM-1, consequently giving a remarkable increase in μ-selectivity (K_i^{δ}/K_i^{μ} of 226 290 and 185 876, respectively), which made analogues **12** and **13** also the most μ-selective analogues. Introduction of (1-naphthyl)Map (**14**) and (2-naphthyl)Map (**15**) to the sequence decreased their binding μ-affinities by 10- to 11-fold, and these analogues displayed similar μ-selectivity compared to the parent peptide.

In Vitro Pharmacological Activity. Pharmacological activities were evaluated in vitro using isolated guinea pig ileum (GPI) for MOR and mouse vas deferens (MVD) for DOR. The former tissues contained predominantly μ-opioid

dx.doi.org/10.1021/jm300664y | J. Med. Chem. 2012, 55, 6224–6236

receptor but also κ-opioid receptor, whereas the latter included predominantly δ-opioid receptor but contained μ- and κ-opioid receptors as well. The potencies of these analogues to inhibit electrically evoked neurotransmitter release and the resulting muscle contractions in GPI and MVD preparations were summarized in Table 2. In the GPI assay, the potency of analogues **7**−**9** and **11** were found to be similar to that of EM-1. In agreement with the radioligand binding affinity assays, analogues **12** and **13** were the two most potent analogues, which exhibited inhibition constants of 2.92 and 3.94 nM, respectively. Analogues **3**, **5**, and **15** with radioligand binding affinities lower than EM-1 showed similar GPI potency as EM-1. Although analogue **8** exhibited slightly decreased affinity toward MOR in radioligand binding assays, its potency was observed to be nearly 2-fold higher in the GPI assays. In MVD assays, all analogues were relatively weak DOR agonists except **4**, **12**, and **13**. The three analogues showed relative potent in MVD potency, though they exhibited low K_i^{δ} values. In order to make clear this discrepancy, the MVD activity of EMs and all the analogues was examined using a specific DOR antagonist, naltrindole. The results showed that the MVD activity of analogues was partly inhibited (23−65%) by naltrindole as well as that of EMs, suggesting the MVD activity of these analogues was mainly produced by the coexisting μ-opioid receptor in the MVD tissues. Such discrepancy between the MVD potency and DOR binding affinity was also observed in previous studies.[34−36]

Inhibition of Forskolin-Stimulated cAMP Increase. It was widely known that inhibition of cAMP production was one of the physiological consequences of agonist binding to the MOR.[37,38] The potencies of the new EM-1 analogues were evaluated via functional [^{3}H]cAMP competitive assays using HEK293 cells expressing MOR.[27,37,38] The results of the analogue stimulated [^{3}H]cAMP functional assays are summarized in Table 3. All of the analogues showed inhibition of forskolin (10 μM) stimulated cAMP production in a concentration-dependent manner. Potency (EC_{50}) and efficacy (E_{max}) values were compared with those of EMs and DAMGO. Analogues **4** and **6**−**13** exhibited higher potencies than EMs, but the replacements proceeded at Trp^3, resulting in analogues **3** and **5** displaying lower potencies than the native peptides. Analogues **12** (EC_{50} = 0.0334 nM) and **13** (EC_{50} = 0.0342 nM) showed about 431 and 421 times higher potency than EM-1 (EC_{50} = 14.4 nM). Endomorphins exhibited comparable potency but lower efficacy (E_{max} of 83.13% and 82.75%, respectively) compared with DAMGO, confirming that the EMs were partial agonist and DAMGO was a full agonist.[39,40] Analogues **4**, **12**, and **13** exhibited the highest efficacies (E_{max} of 97.94%, 97.14%, 98.73%, respectively), acting as full agonists. Analogues **5**−**11**, **14**, and **15** displayed slightly lower efficacy than DAMGO, which indicated that those analogues remained partial agonist properties.

Effect of the Analogues on ERK1/2 Activation by the μ-Opioid Receptor. It had been reported that ERK1/2 phosphorylation could result from MOR activation.[41,42] To examine whether stimulation of the MORs by the analogues had a downstream effect, alteration of ERK1/2 phosphorylation was evaluated in HEK293 cells expressing MOR. Analogues **4**, **12**, and **13** were selected considering their high bioactivity. Serum-starved HEK293 cells stably expressing the MOR were treated with analogues **4**, **12**, and **13** for the times indicated in Figure 1. EM-1 and analogues **4**, **12**, and **13** obviously stimulated ERK1/2 phosphorylation in 10 min in a concentration-dependent manner. Compared with EM-1, all of the tested analogues were able to activate ERK1/2 by stimulating MOR at 10 nM, but the magnitudes of the phosphorylation for analogues **4**, **12**, and **13** were reduced much more slowly than the native EM-1. A statistical difference was observed at 1 pM: the magnitudes of the phosphorylation for analogues **4**, **12**, and **13** were much stronger than that of EM-1, which indicated that the three analogues exhibited higher potencies for ERK1/2 phosphorylation.

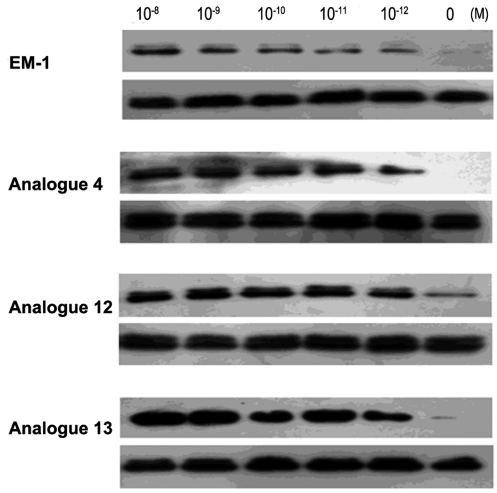

Figure 1. Analogues stimulated pERK1/2 phosphorylation in HEK293 cells expressing human μ-opioid receptor. HEK293 cells stably expressing μ-opioid receptor were treated with analogues **4**, **12**, **13**, and native EM-1 for the indicated concentrations (mole). Whole cell lysates were prepared and analyzed for pERK and ERK content by Western blot. Results are representative of at least three independent experiments.

Antinociception. Antinociceptive potencies of EM-1 and its analogues were studied in the mice tail-flick test. Antinociception was expressed as a percentage of maximum possible effect (% MPE), and analogues **4**, **8**, **12**, and **13** were selected for determination of ED_{50} values based on their potential binding affinities and functional activities (Table 4).

Table 4. In Vivo Antinociceptive Activities of EM-1 and Its Analogues Given icv To Produce Tail-Flick Inhibition in the Mouse

peptide	ED_{50} [a] (nmol/kg)
1	15.2 (13.1−19.3)
4	2.33 (1.74−3.03)
8	9.28 (6.66−12.5)
12	1.42 (1.11−1.88)
13	1.55 (1.09−2.06)

[a]The ED_{50} values were estimated at the time of peak activity and are given as the mean value with its 95% confidence limits.

The ED_{50} value for EM-1 after icv administration was 15.2 nmol/kg, which was in agreement with a previous report.[43] Analogues **4**, **8**, **12**, and **13** displayed a better analgesic effect and produced dose- and time-dependent inhibition at doses ranging from 0.67 to 20 nmol/kg compared with the parent peptide (Figure 2A−E). Analogue **12** displayed the highest analgesic effect, about 10.9-fold more potent than EM-1, and analogues **4**, **8**, and **13** also showed a more potent analgesic effect with ED_{50} values of 1.6- to 9.5-fold higher, respectively.

dx.doi.org/10.1021/jm300664y | J. Med. Chem. 2012, 55, 6224−6236

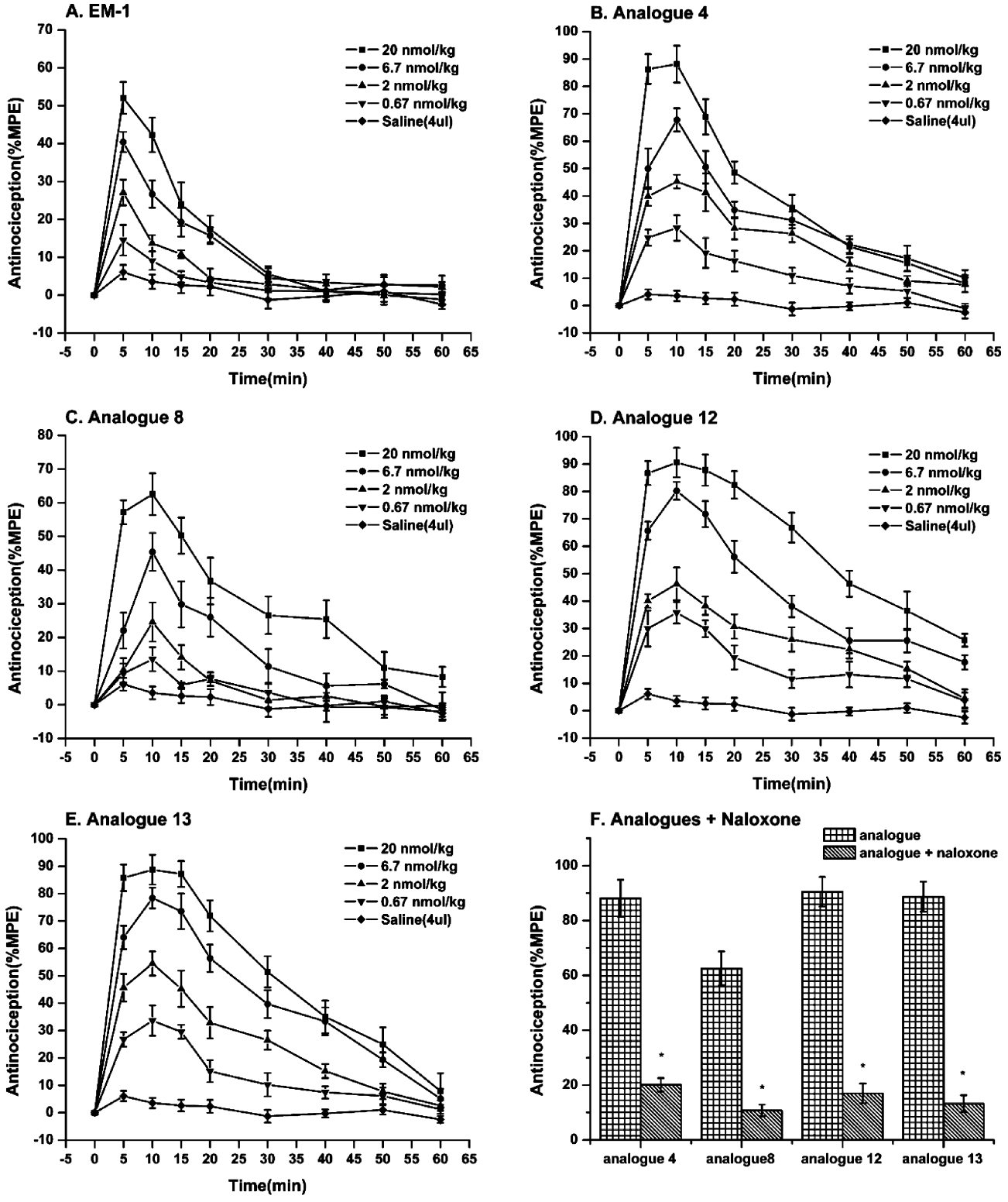

Figure 2. Time course of the antinociceptive effect in icv EM-1 (A) and analogues **4** (B), **8** (C), **12** (D), and **13** (E) in the mouse tail-flick test. Groups of mice were administered an icv injection of saline or different doses of EM-1 and its analogues. The doses used are shown in the figure. The tail-flick responses were measured at 5, 10, 15, 20, 30, 40, 50, and 60 min after the injection. Each value represents the mean ± SEM for 10−15 mice. The icv injection saline versus each dose of the above drugs are significantly different ($p < 0.05$) (Student's t test). The antinociceptive effects induced by EM-1, analogues **4**, **8**, **12**, and **13** at 20 nmol/kg were significantly antagonized by naloxone (2 mg/kg) ($p < 0.05$) (F). Naloxone was administered ip 10 min before icv administration of drugs. The error bar indicates the SEM of the mean, and the asterisk indicates that the response was significantly different from control.

Moreover, antinociceptive effects of analogues **4**, **8**, **12**, and **13** were inhibited by naloxone (2 mg/kg, ip), suggesting that

dx.doi.org/10.1021/jm300664y | J. Med. Chem. 2012, 55, 6224−6236

MOR was involved in producing analgesia (Figure 2F). All the other analogues produced antinociceptive activities in dose-related manner at a dose of 20 nmol/kg (Table S2).

Metabolic Stability. The metabolic stability of EM-1 and its analogues was assessed in mouse brain homogenate. Table 5 summarized the half-lives determined for EM-1 and some of its potent analogues in twice-washed 15% mouse brain membrane homogenate. Within the brain homogenate, EM-1 disappeared rapidly with a half-life of 16.9 min. The replacement of Phe[4] in EM-1 with Map resulted in an enhancement of the stability, giving analogues **4**, **8**, **12**, and **13** the half-life range from 62.2 to 89.9 min. Furthermore, analogue **8** exhibited a significant enhancement of metabolic stability of about 5.3-fold compared with EM-1.

Table 5. Half-Lives of EM-1 and Its Potent Analogues in Mouse-Brain Membrane Homogenate[a]

peptide	$100 \times k$ (min^{-1})[b]	half-life[c]
1	4.10 ± 0.14	16.9 ± 1.2
4	1.11 ± 0.05	62.4 ± 3.1
8	0.77 ± 0.18	89.9 ± 9.3
12	0.81 ± 0.19	85.9 ± 9.2
13	0.78 ± 0.22	88.3 ± 8.2

[a]Values are arithmetic mean of at least three individual experiments ± SEM. The protein content of the brain homogenate was 2.1 mg/mL. [b]Velocity constants. [c]Half-lives were calculated on the basis of pseudo-first-order kinetics of the disappearance of the peptides.

Molecular Modeling. To further investigate the interaction modes between the analogues and receptor, analogues **4**, **5**, and **12** were subjected to molecular docking and molecular dynamics (MD) simulations in view of their biological activities and structural diversity. The three analogues were flexibly docked into a model of human MOR, and then the resultant docking models were further optimized with molecular dynamics. The binding modes of these analogues established after MD simulations were shown in Figure 3. The obtained binding orientation of analogue **4** was similar to that of EM-1 that was reported previously by our group:[44] the Tyr[1] lay at the bottom of the binding site, and its protonated nitrogen moiety interacted with the carboxyl group of Asp147 to form a salt bridge, and the rest of the analogue was orientated toward the extracellular surface. This analogue formed three hydrogen bonds with Thr218, Glu229, and Lys233, respectively. Analogue **4** was also stabilized by many stacking interactions with the aromatic moieties of the receptor. The side chain of Tyr[1] pointed toward a hydrophobic pocket composed mainly of the aromatic residues Tyr148, Phe152, Phe237, and Trp293. The aromatic groups of Trp[3] and (Ph)Map[4] were involved in stacking interactions with the side chains of Phe221 and Trp318. Site-directed mutagenesis experiments had already determined the importance of Asp147, Tyr148, Glu229, H223, and Trp318, and our proposed model was in good agreement with the available mutation studies.[45−51] In addition, our modeling complex shared a similar ligand binding site with the recently resolved crystal structure of human MOR bound to antagonist β-FNA:[52] eight residues (Asp147, Tyr148, Met151, Lys233, Trp293, Ile296, His297, and Val300) that had direct interactions with β-FNA were also found to make close contacts with the analogue (Supporting Information Table S3), indicating that our modeling results were in accordance with the crystal structure. In analogue **5**, Tyr[1] was inserted inside the aromatic clusters of Tyr148, Phe152, Phe237, and Trp293 and formed a salt bridge with Asp147. However, this analogue lost its contact with Phe221, and its interaction with Trp318 was also weakened. In addition, analogue **5** formed only one hydrogen bond, between (Ph)Map[4] and Asp216, with the receptor. Analogue **12** bound in the same aromatic pocket as described for analogue **4** and formed the same hydrophilic interactions with Asp 147, Thr218, and Glu229. Furthermore, the oxygen on the furyl ring of (2-furyl)Map[4] formed two hydrogen bonds with the side chains of His223 and Lys233, respectively.

DISCUSSION

For many peptide hormones and neurotransmitters, peptides could be thought of as being composed of a "message" region and an "address" region. The message sequence was the part of the peptide structure that was necessary for agonist activity and signal transduction. The address region was the part of the structure that was primarily important for recognizing and binding to the receptor. Previous structure−activity relationship (SAR) studies demonstrated that the endomorphin sequence could also be divided into a N-terminal tripeptide message

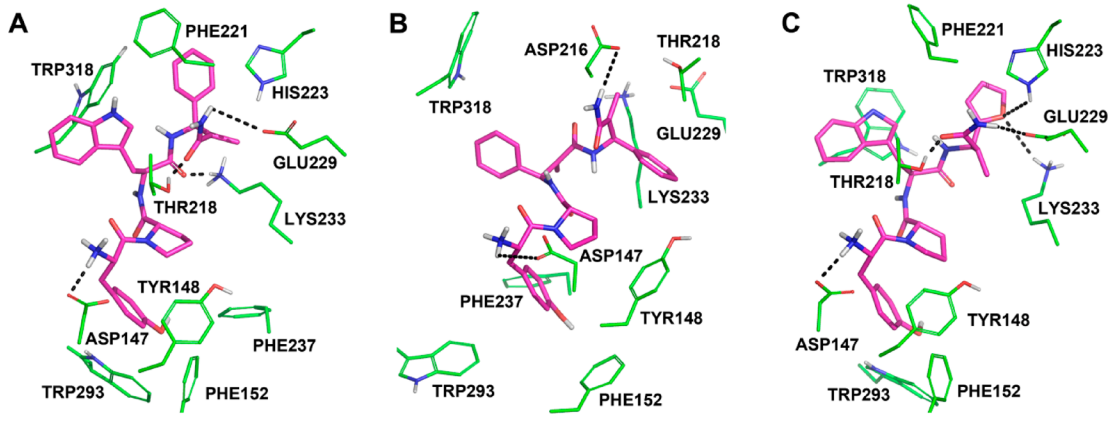

Figure 3. Binding modes of the three peptides obtained after MD simulations optimization: analogue **4** (A), analogue **5** (B), analogue **12** (C). Predicted peptide binding poses are shown in line mode with their carbon atoms in magenta. Residues making close interactions with the peptides are labeled with their carbon atoms in green. Oxygen, nitrogen, and hydrogen atoms are colored as red, blue, and white, respectively. Hydrogen bonds are represented as black dashed lines.

dx.doi.org/10.1021/jm300664y | J. Med. Chem. 2012, 55, 6224−6236

domain (Tyr^1-Pro^2-Phe^3/Trp^3) and a C-terminal address domain (Phe^4-NH_2). C-Terminal residues played an important role in the biological activity of MOR-specific ligands, and many investigators proposed that the C-terminal sequence could help in choosing or stabilizing a favorable conformation among multiple conformations, and it was indispensable for the high binding activity to MOR. In this study, a series of unnatural β-amino acids, 2-methylene-3-aminopropanoic acids (Map), were synthesized and incorporated into EM-1 mainly at the address domain. Compared with classic β-amino acid with flexible backbone, our unnatural amino acid was constrained by introduction of a double bond at the Cα. The introduction of Map into the different positions in the EM-1 resulted in analogues with varied in vitro and in vivo activities.

In our study, the binding affinity and in vitro bioassays indicated that the incorporation of (Ph)Map at position 3 or at positions 3 and 4 simultaneously was detrimental to structural replacement. This is in agreement with previous studies in which substitution of Phe^3/Trp^3 with corresponding β-amino acid resulted in a great decrease of binding affinity.[26,27] Surprisingly, the replacement taken at position 4 led to analogue **4** with remarkable increase in binding affinity and bioactivity, and this analogue also exhibited improvement in μ-selectivity with respect to EM-1. Compared with the β-Phe^4 replacement,[26] (ph)Map^4 primarily constrained the space orientation of the C-terminal amide. The NH_2 group was regarded as an important pharmocophore for determining the activity of EMs.[53,54] Consistent with previous reports our data further emphasized that the space orientation of C-terminal amide also exerted great influence in the regulation of the opioid pharmacological property. In other words, extending the C-terminal backbone structure with appropriate structural constraint would improve the bioactivity of EMs. Analogues **6**−**11**, which contained fluorine, chlorine, methoxyl, or piperonyl group at different positions on the aromatic ring of Map^4, exhibited decreased MOR affinity and selectivity compared with analogue **4**. A similar tendency was observed when incorporation of a subunit with different lipophilicity or electronic character at the third aromatic ring of opioid peptide was shown to be detrimental to the activity of MOR.[35,36,55,56] This data suggested that these kinds of modifications might interfere with the interaction between the aromatic ring of Map^4 and the residues on the receptor. In addition, the binding affinities of analogues **7**−**9** could be found in the order of **8** > **9** > **7**, indicating that the meta-position modification of the phenyl ring might be more favored. Four analogues with heteroaromatic ring at position 4 (analogues **12**−**15**) were also synthesized and evaluated. It was in agreement with previous study that analogues containing a naphthyl ring (**14** and **15**) showed reduced activity.[57−59] Interestingly, **12** and **13** were found to be the most active and selective analogues with incorporation of a furyl ring. These results confirmed that the size and atomic composition of the third aromatic ring could be a very important feature to determine the activity of EM-1. Furthermore, our results also indicated that, compared with phenyl ring, the furyl ring could reinforce the interaction between the peptide and the receptor.

The functional activities of the analogues were determined by measuring the inhibition of forskolin-stimulated cAMP accumulation and phosphorylation of MAPK kinase in HEK293 cells stably expressing the MOR. The [^{3}H]cAMP binding assay results proclaimed that most of the analogues exhibited higher potencies than the parent. Analogues **12** and **13** displayed the highest receptor functional potencies. As we know, stimulation of the MOR by the agonist had a downstream effect to alter the phosphorylation of EKR1/2. It was reported that the phosphorylation of ERK1/2 might contribute to the pain regulation.[60] The tested analogues revealed an increase in ERK1/2 phosphorylation by stimulating MOR in 10 min in a concentration-dependent manner. Rapid ERK1/2 phosphorylation was compared among all the tested peptides. All tested analogues showed significant increase in ERK1/2 phosphorylation at 1 pM, which was parallel to inhibition of cAMP accumulation and binding affinity assays. The cAMP accumulation and ERK1/2 phosphorylation results suggested that the C-terminal group of EMs had a profound influence on the activation state of MOR.

The antinociceptive activities of peptides were assessed by the tail-flick test after icv injection. Most of the analogues express approximate or even higher analgesic potency and extension of acting time. That was probably related to their high efficacy to the MOR. In addition, it was possible that the enhanced stability in brain homogenate also contributed to the increase of in vivo activities, since this factor might lead to a longer duration of the peptide in the brain. Furthermore, it had been reported that a variety of enzymes were involved in peptide degradation. Carboxypeptidase Y and proteinase A could reveal deamidase activity, hydrolyzing the endomorphins into peptide acids, and then cleave off the C-terminal Phe.[10] Insertion of Map into position 4 probably impeded these proteases from recognizing the cleavage site.

Computational studies were performed to understand the interaction characteristics of these analogues. The analysis through the results of molecular docking and molecular dynamics simulations of the ligand−receptor systems suggested a good agreement between our study and the site-directed mutagenesis data. We found that the interaction between the C-terminal and the receptor could be essential for the binding affinities of these analogues. For analogues **4** and **12**, close interactions with the receptor was observed and both of their C-terminal residues formed hydrogen bonds with Thr218 and Glu229. It was noteworthy that the incorporation of a furyl ring into the C-terminal residue (analogue **12**) further stabilized the peptide conformation. The oxygen on the furyl ring could act as a hydrogen acceptor and therefore form two hydrogen bonds with His223 and Lys233, respectively. In a binding pose of analogue **4**, His223 was not involved in any hydrogen bond with the analogue and Lys233 was used to contact with Trp^3 as well. These results indicated that introducing a pharmacophore feature of a hydrogen bond acceptor into the C-terminal residue might enhance the interaction between the peptide and the receptor. For analogue **5**, the C-terminal residue lost its contact with the residues mentioned above on the receptor but formed a hydrogen bond with Asp216. The aromatic interaction between analogue **5** and the receptor was also weak. As a result, this analogue did not have sufficient interactions with the receptor. Taking the binding affinities into consideration, we presumed that the binding pocket formed by Thr218, His223, Glu229, and Lys233 might be responsible for the binding of the C-terminal sequence of endomorphin peptide. This polar moiety probably anchored the address domain of the peptide at the right position inside the receptor so that the peptide could have close interactions with the receptor.

CONCLUSIONS

In the present study, we developed a class of highly potent MOR agonists by incorporating conformational constrained unnatural β-amino acids (2-methylene-3-aminopropanoic acids (Map)) into EM-1. From a combination of multiple in vitro and in vivo assays, we found that Map would facilitate the interaction between the analogues and the receptor when they were placed in the C-terminal region of EM-1. Besides, the bioactivity of these analogues varied when the side chain element of Map changed. Analogues **12** (H-Tyr-Pro-Trp-(2-Furyl)Map-NH_2) and **13** (H-Tyr-Pro-Trp-(3-Furyl)Map-NH_2) behaved as the most active agonists. In binding affinity assays they exhibited extraordinary affinities compared with the EM-1 and were even ~431 times more potent in the inhibition of forskolin-stimulated cAMP accumulation. These analogues also displayed increased metabolic stability in mouse brain homogenate. In vivo assays proved that these two analogues showed enhanced antinociceptive activities. Overall, the present study demonstrated that the modification used in this research was successful for increasing the bioactivity of EM-1, and these analogues might be of great importance in potential application as drug candidates as analgesic for pain relief.

EXPERIMENTAL SECTION

Materials and Methods. Mass spectra were measured with a Maxis 4G ESI-TOF analyzer (Bruker, U.S.). Melting points were determined on a micromelting point apparatus (AII-E, China). Optical rotations were determined with AUTOPOL IV (Rudolph Research Analytical). Purities were determined by ascending TLC performed on precoated plates and by analytical RP-HPLC. The purity of the analogues was confirmed by ascending TLC performed on precoated plates (silica gel 60 F254, Yinlong, China) in the following solvent systems (all v/v): (I) ethyl acetate−methanol−ammonia water (30:10:1) and (II) acetone−glacial acetic acid−water (8:1:1). UV light and I_2 vapor were applied to visualize the TLC spots. Analytical RP-HPLC was carried out with a Waters Delta 600 instrument equipped with a Waters Deltapak C18 column (4.6 mm × 250 mm, 5 μm). Absorbance was monitored at λ = 220 nm. The solvents for analytical RP-HPLC were as follows: A, 0.05% TFA in acetonitrile; B, 0.05% TFA in water. The column was eluted at a flow rate of 1 mL/min with a linear gradient of A/B = 10:90 to A/B = 90:10 for 30 min and a gradient of A/B = 90:10 to A/B = 10:90 for 5 min. The retention time was reported as t_R (min). The final purity of the analogues was ≥95%. The detailed analytical properties of the synthetic analogues are provided in Table S1 in the Supporting Information.

Guinea pigs (300−350 g, National Institute of the Biological Products, Gansu, People's Republic of China) were used for guinea pig ileum (GPI) assay. Male Kunming mice (30−35 g, Animal Center of Medical College of Lanzhou University, Gansu, People's Republic of China) were used for mouse vas deferens (MVD) assay. Male Kunming mice (18−22 g, Animal Center of Medical College of Lanzhou University, Gansu, People's Republic of China) were employed for analgesia studies. They were housed in a temperature-controlled environment (22 ± 2 °C) under standard 12 h light/dark conditions and received food and water ad libitum. All animals were cared for, and experiments were carried out in accordance with the principles and guidelines of the American Council on Animal Care. All protocols were approved by the Ethics Committee of Lanzhou Medical College.

[^{3}H]DAMGO (50 Ci/mmol), [^{3}H]DPDPE (43 Ci/mmol), and [^{3}H] cAMP (50 Ci/mmol) were purchased from Perkin-Elmer, Boston, MA. Anti-phospho-ERK1/2 (Thr202/Tyr204) antibodies, anti-ERK1/2 antibodies, and HRP-conjugated secondary antibody were purchased from Cell Signaling Technology Inc. Protein kinase A, forskolin, and IBMX were the products of Sigma-Aldrich (St. Louis, MO, U.S.). The radioactivities were measured by a Perkin-Elmer 2460 microplate counter. The scintillation cocktail was obtained from Perkin-Elmer, Boston, MA.

General Procedure for Synthesis of the Boc Protected Unnatural Amino Acid Map (Boc-Map-OH). Boc-Map-OH was derived from our group's published product.[30] HWE reagent (325.2 mg, 1.5 mmol) and catalyst (87.6 mg, 0.2 mmol, 20 mol %) were dissolved in toluene (10 mL) at 0 °C. Then α-amidosulfones (1 mmol) were added followed by addition of an aqueous solution of K_2CO_3 (1.5 M, 0.8 mL). After the reaction was finished, the intermediate product was quickly isolated use column chromatography (PE/EA = 1:1). Then it was dissolved in THF (6 mL) and added to a precooled solution of MeONa (2.2 equiv) in MeOH (2 mL) slowly at −15 °C. After the mixture was stirred for 30 min, paraformaldehyde (5 equiv) was added, and the mixture was stirred for another 8 h. The reaction process was monitored by TLC. When the reaction was completed, saturated aqueous NaCl was added and extraction was with ethyl acetate. Drying was over Na_2SO_4. After evaporation of the solvents, the residue was purified on a silica gel column (PE/EA = 7:1). Then the corresponding intermediate product was dissolved in THF (5 mL) at 0 °C and added to an aqueous solution of LiOH (1M, 2.5 mL). The mixture was stirred at the room temperature for 12 h. Upon completion, the mixture was extracted with DCM and dried over Na_2SO_4. After concentration of the solvents, the residue was purified on a silica gel column (PE/EA = 1:2) to give the corresponding product.

Peptide Synthesis. Endomorphins and their analogues were obtained by solution-phase methods with segment-coupling peptide synthesis strategy. Synthesis of all the peptides that contain the Map residue has been accomplished by performing an active ester reaction with the EDC/HOBt coupling method. The first step in the synthesis of all the analogues involved the preparation of the amide of the unnatural amino acid Map, which was easily achieved by EDC/HOBt coupling with ammonia. Then the N-terminal dipeptide (Boc-Tyr-Pro-OH) and C-terminal dipeptide (Boc-Trp-Map-NH_2, Boc-Map-Phe-NH_2, or Boc-Map-Map-NH_2) were obtained by the same method. After synthesis of fragments, the active ester method with EDC/HOBt as the coupling agent was performed with N- and C-terminal fragments coupling. All the intermediates were characterized by TLC, ^{1}H NMR, and ESI-TOF MS. Deprotection of Boc was performed using HCl/EA, and final products were purified by semipreparative RP-HPLC.

Synthesis of Boc-Tyr-Pro-OH. A solution of Boc-Tyr-OH (10 mmol, 2.81 g), DCC (12 mmol, 2.472 g), and HOSu (12 mmol, 1.38 g) in distilled THF (50 mL) was stirred at 0 °C. H-Pro-OH (1.2 mmol, 1.38 g) was dissolved in saturated aqueous $NaHCO_3$, adjusting the pH to 9−10, and then the reaction mixture containing Boc-Tyr-OSu and H-Pro-ONa was stirred at 0 °C for 30 min and at room temperature overnight. When the reaction was completed, the appropriate portion was extracted with THF. The extract was washed successively with 5% citrate acid (10 mL), twice, and brine, dried over Na_2SO_4, and evaporated at reduced pressure.The residue was purified on a silica gel column (EA/MeOH = 10:1). Yield: 3.24 g (86%). R_f = 0.38 (PE/EA/HOAc = 10:20:1). $[\alpha]^{20}_D$ −18.3 (c 1.0, MeOH). Mp: 103−106 °C. ESI-TOF MS: m/z [M + H$^+$] calcd, 379; found, 379.2.

General Procedure for the Synthesis of Boc-Trp-Map-NH_2. A solution of Boc-Trp-OH (10 mmol, 3.04 g), EDCI (16 mmol, 3.072 g), HOBt (14.5 mmol, 1.96 g), and DIEA (40 mmol, 6.50 mL) in distilled DCM (50 mL) was stirred at 0 °C. Then H-Map-NH_2 (1.2 mmol) dissolved in distilled DCM (10 mL) was added slowly into the mixture, and the mixture was stirred at 0 °C for 30 min and at room temperature overnight. When the reaction was completed, the appropriate portion was extracted with DCM. The extract was washed successively with 5% citrate acid (10 mL), saturated $NaHCO_3$ (10 mL), twice, and brine, dried over Na_2SO_4, and evaporated at reduced pressure. The residue was purified on a silica gel column (DCM/MeOH = 15:1) with a yield of 75−90%.

General Procedure for the Synthesis of H-Tyr-Pro-Trp-Map-NH_2. A solution of N-terminal fragments Boc-Tyr-Pro-OH (1.0 mmol, 0.38 g), EDCI (1.6 mmol, 0.31 g), HOBt (1.45 mmol, 0.19 g), and DIEA(4.0 mmol, 0.66 mL) in distilled DCM (10 mL) was stirred at 0

dx.doi.org/10.1021/jm300664y | J. Med. Chem. 2012, 55, 6224−6236

°C. Deprotection of the Boc groups of C-terminal fragments (1.2 mmol) was performed with HCl/EA (1:4, v/v). Then the reaction mixture containing Boc-Tyr-Pro-OBt and deprotected C-terminal fragments H-Trp-Map-NH_2 was stirred in distilled DCM at 0 °C for 30 min and at room temperature overnight. When the reaction was completed, it was extracted with DCM. The extract was washed successively with 5% citrate acid (10 mL), saturated $NaHCO_3$ (10 mL), twice, and brine, dried over Na_2SO_4, and evaporated at reduced pressure. The crude protected tetrapeptides residue was purified on a silica gel column (EA/MeOH = 15:1) with a yield of 60−80%.

The Boc-group deprotection was performed by treatment with HCl/EA (1:4, v/v) at room temperature for 2 h. After extraction with DCM/MeOH = 10:1, the solvent was evaporated at reduced pressure. The residue was purified by semipreparative RP-HPLC and characterized by TLC, TOF-MS, $[\alpha]^{D}_{20}$, mp, and RP-HPLC, which revealed that all the peptides were the desired peptides with 95−99% purity. Data are reported in Table S1 in the Supporting Information.

Establishment of HEK293 Cells Stably Expressing μ- or δ-Opioid Receptor. HEK293 cells were cultured in Dulbecco's modified Eagle's medium (DMEM) supplemented with 10% fetal calf serum. The eukaryotic vector, pcDNA3.1-FLAG-μ-OR or pcDNA3.1-Myc-δ-OR, was introduced into HEK293 cells by Lipofectmine2000 according to the manufacturer's instruction. The day after transfection, G418 (800 μg/mL) was added to the medium for 2 weeks. Then the antibiotic-resistant clones derived from a single cell were selected and further characterized by RT-PCR and Western blotting to ensure the expression of human MOR or DOR. The cellular function of MOR or DOR was confirmed by the μ-opioid receptor antagonist naloxone and δ-opioid receptor antagonist naltrexone. Briefly, HEK293-μ-OR or HEK293-δ-OR cells were preincubated with or without 1 μM naloxone or 1 μM naltrexone in DMEM medium for 30 min. Then the cells were stimulated using 1 μM EM-1 or 1 μM DPDPE and 10 μM forskolin to measure the cAMP accumulation level.

Cell Culture. HEK293 cells stably expressing either the FLAG-tagged μ-opioid receptor or the Myc-tagged δ-opioid receptor were grown in Dulbecco's modified Eagle's medium (DMEM) supplemented with 10% fetal calf serum, 100 units/mL penicillin, and 0.1 mg/mL streptomycin at 37 °C in a humidified atmosphere containing 5% CO_2 as described.[61]

Radioligand Binding Assay. In the experiments designed to define peptide specificity for μ- and δ-opioid receptors, whole cells expressing either MOR or DOR ($(2.5-3.5) \times 10^6$ cells/tube) were incubated with 1.7 nM [^{3}H]DAMGO or 1.0 nM [^{3}H]DPDPE and $10^{-10}-10^{-4}$ M unlabeled ligands for each experiment. Nonspecific binding was measured in the presence of 10 μM naloxone or 10 μM naltrexone. The reaction was performed at 25 °C for 60 min in freshly prepared binding buffer (25 mM Hepes, 5 mM $MgCl_2$, 1 mM $CaCl_2$, 2.5 mM ethylenediaminetetraacetic acid [EDTA], and 0.4% bovine serum albumin [BSA], pH 7.4).[62,63] The reaction was stopped by rapid vacuum filtration through GF/C filters (Whatman, Maidstone, U.K.) using a cell harvester. The filters were washed twice with 6 mL of ice-cold buffer and then dried for 1 h at 80 °C. The radioactivity was measured by liquid scintillation counting (liquid scintillation counter, PerkinElmer). The affinity constants (K_i) were calculated according to Cheng and Prusoff with GraphPad Prism 5.0 software (GraphPad Software Inc., San Diego, CA). The dissociation constant (K_d^{μ} = 0.6 nM, K_d^{δ} = 2.8 nM) and the number of binding sites (B_{max}) were calculated by Scatchard analysis using at least seven concentrations of [^{3}H]DAMGO or [^{3}H]DPDPE in the range 0.085−8.5 or 0.10−5.05 nM. Nonspecific binding was assessed in the presence of 10 μM naloxone and 10 μM naltrexone.

Measurements of cAMP Accumulation. Measurements of adenylyl cyclase activity were performed as described in the literature.[64−67] Briefly, the day before the assay, HEK293 cells stably expressing the μ-opioid receptor were seeded at 80% confluency in 24-well microtiter plates. Before the start of the assay, the culture medium was aspirated and each well was washed twice with serum-free medium warmed to 37 °C. Then 400 μL of prewarmed serum-free medium containing 1 mM IBMX was added to each well and incubated for 10 min at 37 °C. An amount of 100 μL of serum-free medium containing various concentrations of the appropriate ligand (5×10^{-11} M to 5×10^{-5} M) using 50 μM forskolin was added to the cells, and the samples were incubated at 37 °C for 30 min. They were removed from the medium. Then 0.2 N HCl was added to the cells at room temperature for 30 min. The clarified lysates were neutralized with 10 N NaOH. Lysates were transferred to microcentrifuge tubes and microcentrifuged 2 min at top speed at room temperature. Then 50 μL of neutralized lysates, 100 μL of PKA (60 μg/mL), and 50 μL of [^{3}H]cAMP were mixed briefly and incubated for ≥2 h at 4 °C. The chilled charcoal suspension was added to adsorb free cAMP from solutions. An amount of 200 μL of the supernatant was transferred to a scintillation vial. Scintillation fluid was added, and radioactivity was quantified in a scintillation counter (liquid scintillation counter, PerkinElmer). Analysis of the data was performed using the GraphPad Prism software (version 5.0, San Diego, CA).

Detection of MAPK Phosphorylation. ERK phosphorylation was measured by immunoblotting as described.[68−70] HEK293 cells stably expressing the FLAG-tagged μ-opioid receptor were seeded in 12-well plates. At 16 h before the addition of the ligands, the culture medium was removed and replaced by fresh serum-free medium. For rapid ERK1/2 phosphorylation assay, the cells were treated with EM-1, **4**, **12**, and **13** at different concentrations and incubated at 37 °C for 10 min. Cell monolayers were rinsed with ice-cold PBS, and whole lysates were prepared by the addition of RIPA lysis buffer containing 10 μM PMSF and phosphatase inhibitor cochtails (P5726, Sigma-Aldrich) for 5 min. Soluble proteins were separated by centrifugation at 15 000 rpm for 10 min. Protein concentration was determined by using BCA protein assay kit (Pierce, Thermo Scientific, U.S.). A total amount of 20 μg of protein from each sample was prepared for 10% SDS−polyacrylamide gel electrophoresis and electroblotted onto polyvinylidene difluoride membranes. Membranes were probed with primary antibody against phosphor-ERK1/2 or ERK1/2 (1:1000 dilution in blocking solution, Cell Signaling Technology Inc.). Immunoreactive proteins were visualized using a horseradish peroxidase sensitive ECL chemiluminescent Western blotting kit (Pierce, Thermo Scientific, U.S.).

In Vitro Assays on Isolate Tissue Preparation. In vitro opioid activities of peptides were tested in the guinea pig ileum (GPI) and mouse vas deferens (MVD) bioassays as reported elsewhere. For the GPI assay, the myenteric plexus longitudinal muscle was obtained from guinea pig (300−350 g, National Institute of the Biological Products, Gansu, People's Republic of China) as described by Rang.[31] For the MVD assay, the vas deferens of male Kunming strain mice (30−35 g, Animal Center of Medical College of Lanzhou University, Gansu, People's Republic of China) was prepared as described by Hughes et al.[32] The GPI tissue and MVD tissues were mounted in a 10 mL bath containing aerated 95% O_2, 5% CO_2 with Krebs−Henseleit solution at 37 and 36 °C, respectively. Both tissues were used for field stimulation with bipolar rectangular pulses of supramaximal voltage. Dose−response curves were constructed, and IC_{50} values (concentration causing a 50% decrease in electrically induced twitches) were calculated graphically. Moreover, in both assays, three to four washings were done at intervals of 15 min between each dose. The values were the arithmetic mean of 10−15 measurements. In order to measure whether δ-opioid-receptor-mediated antagonism occurred in the MVD, naltrindole, a selective δ-receptor antagonist, was added to the tissue preparation after 5 min of incubation, the test analogue was added at the IC_{50} dose value, and the percentage recovery (reversal rate) of electrically evoked contraction was then calculated.[35]

Antinociception Test. Antinociceptive responses were determined using the warm water tail-flick test. For the analgesia studies, male Kunming mice weighing 18−22 g were employed. They were obtained from the Animal Center of Medical College of Lanzhou University. Various doses of drugs were injected icv according to the procedure adopted by Haley and McCormick, and the warm water tail-flick responses were measured at different times after the injection. Nociception was evoked by immersing the mouse tail in hot water (50 ± 0.2 °C) and measuring the latency to withdrawal. Before treatment, each mouse was tested, the latency to tail-flick [control latency (CL)]

was recorded, and selection was the one at approximately 3−5 s. The latency to tail-flick was defined as the test latency (TL). The corresponding cutoff time TL was set at 10 s, and 0.9% saline was used as control. The antinociceptive response was expressed as percentage of maximal possible effect (% MPE), calculated by the following equation: % MPE = 100 × (TL − CL)/(10 − CL). The ED_{50} values and their 95% confidence limits were determined by using the graded dose−response procedure.

Metabolic Stability. Mouse brain homogenate was used for enzymatic degradation studies. The 15% mouse brain homogenate was prepared as described previously.[71] Protein content of the suspension was confirmed by BCA potein assay kit (Thermo, Rockford, IL, U.S.). A final protein concentration of 2.1 mg/mL in 50 mM Tris buffer, pH 7.4, was used for all incubations. RP-HPLC analysis determined the stability of peptides. Approximately 10 μL of peptide stock solution was digested with 190 μL of rat brain homogenate at 37 °C in a final volume of 200 μL for incubation. An amount of 20 μL of the aliquots was withdrawn from the mixture at 0, 5, 10, 15, 30, 60, 120, 240 min, and 90 μL of acetonitrile was added immediately for precipitated proteins, placing the tube on ice for 5 min and addeding 90 μL of 0.5% acetic acid at the required time to prevent further enzymatic breakdown. The aliquots were centrifuged at 13000*g* for 15 min at 4 °C. The obtained supernatants were filtered with filters of 0.22 μm, and 50 μL of the filtrate was analyzed by RP-HPLC on a Waters Delta Pak C18 column (4.6 mm × 250 mm, Milford, MA), using the solvent system of 0.05% TFA in acetonitrile (A) and 0.05% TFA in water (B) with a linear gradient of A/B = 10:90 to A/B = 90:10 for 30 min and A/B = 90:10 to A/B = 10:90 for 5 min. The column was eluted at a flow rate of 0.8 mL/min. The degradation rate constants (k) were determined by least-squares linear regression analysis of logarithmic tetrapeptide peak area $[(\ln(A_t/A_0)]$ vs time courses, with at least five time points. The rate constants obtained were used to establish the degradation half-lives ($t_{1/2}$) as ln 2/k.

Molecular Modeling. Using the homology modeling method, Mosberg had reported a kind of MOR model based on the bovine rhodopsin structure,[49] and we also constructed a homology MOR using the same template.[72] By comparison of the two models, it was found that the model built by Mosberg et al. was more suitable for docking peptide agonists because structural alterations were incorporated into this model to obtain an active state receptor structure. Recently, the crystal structure of human MOR was resolved with antagonist β-FNA.[52] The Mosberg model showed a good agreement with the crystal structure. Both structures represented exposed binding pockets that would facilitate the ligand binding process. Moreover, the overall Cα root-mean-square deviation (rmsd) between the two structures was 3.64 Å, indicating that the computational model preserved the main structural architecture of MOR. Considering that the crystal structure probably represented an "inactive state" of MOR, the Mosberg "active" MOR model was chosen as the working receptor model.[49] The model was then refined using 15 ns MD simulations in the phospholipid bilayer. The receptor was inserted into a pre-equilibrated 70 Å × 70 Å DPPC bilayer slab, and the protein membrane system was embedded in a SPC water box. Counterions were added to the system in order to produce a neutral charge on it. MD simulations were performed with the GROMACS 3.3.3 package employing NPT and periodic boundary conditions.[73] A modification of GROMOS87 force field was applied for protein and the lipid.[74] A twin cutoff of 9 Å was used for the short-range interaction, and a cutoff of 12 Å was used for the Lennard-Jones interaction. Particle Mesh Ewald algorithm was used for the calculation of electrostatic contributions to energies and forces.[75] Bond length was constrained using the LINCS algorithm.[76] The systems were coupled to a temperature bath at 300 K, with a coupling constant of 0.1 ps. Semiisotropic coupling with a time constant of 1 ps was applied to keep the pressure at 1.0 bar.[77] The system was first energy-minimized using the steepest descent integrator for 5000 steps. Then a progression of position restraint was performed for 300 ps. Finally, a 15 ns simulation was performed with a time step of 2 fs. The root-mean-square deviation was calculated for the backbone atoms of MOR. The receptor became stable after approximately 7.5 ns (Figure 2). The average structure of the last 1 ns trajectory was considered as the typical structure of the MD simulations.

The molecular dockings were performed with AUTODOCK4.[78] This program suite uses an automated docking approach that allows ligand flexibility, and it employs the Lamarckian genetic algorithm to treat the ligand−receptor interaction. The initial conformations of the three analogues were built based on the NMR structure of endomorphins that we solved previously,[79] and the amide group of Tyr^1 was protonated. Partial charges, necessary for the docking protocol, were assigned according to the Gasteiger−Marsili scheme. The grid maps representing the opioid receptors in the docking process were calculated with AutoGrid. The docking process was performed in two steps.[80,81] First, a box of 42 Å × 42 Å × 42 Å, centered on one of the oxygen atoms of the Asp147, was used with a grid resolution of 5.5 Å. The initial position of the ligand was random. The population size was 100. The maximum number of generations was 27 000, and the maximum number of energy evaluations was 2 500 000. The lowest docking energy conformations or the lowest docking energy conformations included in the largest cluster were considered to be the most stable orientations. In the second step, a box of 40 Å × 30 Å × 50 Å centered on the best conformations obtained in the first step was used with a resolution of 0.3 Å. The number of energy evaluations was changed to 25 000 000, and the population size was raised to 500. The resulting orientations were scored based on the docking and binding energies and on the distance of Asp147 to the protonated nitrogen of the ligand. The docked energies were calculated using a modified scoring function.[82] Experimental studies suggested that the protonated nitrogen moiety interacts with the carboxyl group of Asp147 to form a putative salt bridge and this residue mutated to Ala/Asn or Glu, leading to diminished binding affinities. This residue was believed to be the primary binding site.[45] In the next stage of the study, MD simulations of the all the docking models were performed using the GROMACS program to get more reasonable ligand−receptor binding modes, where the flexibility of the receptor was considered. Each ligand−receptor complex was subjected to a 5 ns MD simulation in the previously described membrane bilayer. The topologies of the ligands were generated by PRODRG.[83] The time evolutions of the rmsd of Cα and total energy were analyzed to evaluate the stability of each system. As shown in Supporting Information Figures S1 and S2, all systems became stable after about 3 ns of MD simulations. Figures were drawn by the means of PyMOL.[84]

Data Analysis. The data are expressed as the mean ± SEM. Responses were analyzed with a one-way ANOVA followed by Dunnett's test for comparison of multiple groups with one saline control group and by Student's t test for comparisons between two groups. $p < 0.05$ was used as the statistical significance level.

■ ASSOCIATED CONTENT

Ⓢ Supporting Information

Experimental details and characterization data for new analogues. This material is available free of charge via the Internet at http://pubs.acs.org.

■ AUTHOR INFORMATION

Corresponding Author

*Phone: +86-9318912567. E-mail: wangrui@lzu.edu.cn.

Author Contributions

§These authors contributed equally.

Notes

The authors declare no competing financial interest.

The manuscript was written with contributions from all authors. All authors have given approval to the final version of the manuscript.

■ ACKNOWLEDGMENTS

We are grateful for the grants from the National Natural Science Foundation of China (Grants 90813012 and

20932003), the Key National S&T Program "Major New Drug Development" of the Ministry of Science and Technology (Grant 2012ZX09504001-003), and Fundamental Research Funds for the Central Universities (Grant lzujbky-2011-86). We acknowledge computing resources and time on the Gansu Supercomputing Center, Cold and Arid Environment and Engineering Research Institute of Chinese Academy of Sciences.

■ ABBREVIATIONS USED

Boc, *tert*-butyloxycarbonyl; DAMGO, H-Tyr-D-Ala-Gly-NMe-Phe-Gly-ol; DCM, dichloromethane; DIEA, *N*,*N*′-diisopropylethylamine; DMF, dimethylformamide; DMSO, dimethyl sulfoxide; DOR, δ opioid receptor; DPDPE, Tyr-*c*(D-Pen-Gly-Phe-D-Pen); ED_{50}, median effective dose; EDC, *N*-ethyl-*N*′-(3-dimethylaminopropyl)carbodiimide; EM-1, endomorphin-1; EM-2, endomorphin-2; ESI-TOF MS, electrospray ionization time-of-flight mass spectrometry; GPI, guinea pig ileum; HOBt, 1-hydroxybenzotriazole; IC_{50}, 50% inhibitory concentration; icv, intracerebroventricular (dosing); ip, intraperitoneally; KOR, κ opioid receptor; MD molecular dynamics; MOR, μ opioid receptor; MVD, mouse vas deferens; RP HPLC, reversed-phase high performance liquid chromatography; THF, tetrahydrofuran; TLC, thin-layer chromatography

■ REFERENCES

(1) Holden, J. E.; Jeong, Y.; Forrest, J. M. The endogenous opioid system and clinical pain management. *AACN Clin. Issues* **2005**, *16*, 291−301.
(2) Lord, J. A.; Waterfield, A. A.; Hughes, J.; Kosterlitz, H. W. Endogenous opioid peptides: multiple agonists and receptors. *Nature* **1977**, *267*, 495−499.
(3) Bodnar, R. J. Endogenous opiates and behavior: 2010. *Peptides* **2011**, *32*, 2522−2552.
(4) Zadina, J. E.; Hackler, L.; Ge, L. J.; Kastin, A. J. A potent and selective endogenous agonist for the mu-opiate receptor. *Nature* **1997**, *386*, 499−502.
(5) Hackler, L.; Zadina, J. E.; Ge, L. J.; Kastin, A. J. Isolation of relatively large amounts of endomorphin-1 and endomorphin-2 from human brain cortex. *Peptides* **1997**, *18*, 1635−1639.
(6) Wilson, A. M.; Soignier, R. D.; Zadina, J. E.; Kastin, A. J.; Nores, W. L.; Olson, R. D.; Olson, G. A. Dissociation of analgesic and rewarding effects of endomorphin-1 in rats. *Peptides* **2000**, *21*, 1871−1874.
(7) Czapla, M. A.; Gozal, D.; Alea, O. A.; Beckerman, R. C.; Zadina, J. E. Differential cardiorespiratory effects of endomorphin 1, endomorphin 2, DAMGO, and morphine. *Am. J. Respir. Crit. Care Med.* **2000**, *162*, 994−999.
(8) Janecka, A.; Fichna, J.; Janecki, T. Opioid receptors and their ligands. *Curr. Top. Med. Chem.* **2004**, *4*, 1−17.
(9) Liu, W. X.; Wang, R. Endomorphins: potential roles and therapeutic indications in the development of opioid peptide analgesic drugs. *Med. Res. Rev.* **2012**, *32*, 536−580.
(10) Tomboly, C.; Peter, A.; Toth, G. In vitro quantitative study of the degradation of endomorphins. *Peptides* **2002**, *23*, 1573−1580.
(11) Cardillo, G.; Gentilucci, L.; Tolomelli, A. Unusual amino acids: synthesis and introduction into naturally occurring peptides and biologically active analogues. *Mini-Rev. Med. Chem.* **2006**, *6*, 293−304.
(12) Schwyzer, R. ACTH: a short introductory review. *Ann. N.Y. Acad. Sci.* **1977**, *297*, 3−26.
(13) In, Y.; Minoura, K.; Ohishi, H.; Minakata, H.; Kamigauchi, M.; Sugiura, M.; Ishida, T. Conformational comparison of mu-selective endomorphin-2 with its C-terminal free acid in DMSO solution, by ^{1}H NMR spectroscopy and molecular modeling calculation. *J. Pept. Res.* **2001**, *58*, 399−412.
(14) Berezowska, I.; Chung, N. N.; Lemieux, C.; Wilkes, B. C.; Schiller, P. W. Agonist vs antagonist behavior of delta opioid peptides containing novel phenylalanine analogues in place of Tyr(1). *J. Med. Chem.* **2009**, *52*, 6941−6945.
(15) Janecka, A.; Kruszynski, R. Conformationally restricted peptides as tools in opioid receptor studies. *Curr. Med. Chem.* **2005**, *12*, 471−481.
(16) Janecka, A.; Staniszewska, R.; Fichna, J. Endomorphin analogs. *Curr. Med. Chem.* **2007**, *14*, 3201−3208.
(17) Tomboly, C.; Ballet, S.; Feytens, D.; Kover, K. E.; Borics, A.; Lovas, S.; Al-Khrasani, M.; Furst, Z.; Toth, G.; Benyhe, S.; Tourwe, D. Endomorphin-2 with a beta-turn backbone constraint retains the potent micro-opioid receptor agonist properties. *J. Med. Chem.* **2008**, *51*, 173−177.
(18) Hruby, V. J.; Balse, P. M. Conformational and topographical considerations in designing agonist peptidomimetics from peptide leads. *Curr. Med. Chem.* **2000**, *7*, 945−970.
(19) Gentilucci, L.; Tolomelli, A. Recent advances in the investigation of the bioactive conformation of peptides active at the micro-opioid receptor. Conformational analysis of endomorphins. *Curr. Top. Med. Chem.* **2004**, *4*, 105−121.
(20) Schiller, P. W. Bi- or multifunctional opioid peptide drugs. *Life Sci.* **2010**, *86*, 598−603.
(21) Seebach, D.; Overhand, M.; Kühnle, F.; Martinoni, B.; Oberer, L.; Hommel, U.; Widmer, H. β-Peptides: Synthesis by Arndt−Eistert homologation with concomitant peptide coupling. Structure determination by NMR and CD spectroscopy and by X-ray crystallography. Helical secondary structure of a β-hexapeptide in solution and its stability towards pepsin. *Helv. Chim. Acta* **1996**, *79*, 913−941.
(22) Appella, D. H.; Christianson, L. A.; Karle, I. L.; Powell, D. R.; Gellman, S. H. β-Peptide foldamers: robust helix formation in a new family of β-amino acid oligomers. *J. Am. Chem. Soc.* **1996**, *118*, 13071−13072.
(23) Steer, D. L.; Lew, R. A.; Perlmutter, P.; Smith, A. I.; Aguilar, M. I. Beta-amino acids: versatile peptidomimetics. *Curr. Med. Chem.* **2002**, *9*, 811−822.
(24) Cheng, R. P.; Gellman, S. H.; DeGrado, W. F. beta-Peptides: from structure to function. *Chem. Rev.* **2001**, *101*, 3219−3232.
(25) Frackenpohl, J.; Arvidsson, P. I.; Schreiber, J. V.; Seebach, D. The outstanding biological stability of beta- and gamma-peptides toward proteolytic enzymes: an in vitro investigation with fifteen peptidases. *ChemBioChem* **2001**, *2*, 445−455.
(26) Cardillo, G.; Gentilucci, L.; Melchiorre, P.; Spampinato, S. Synthesis and binding activity of endomorphin-1 analogues containing beta-amino acids. *Bioorg. Med. Chem. Lett.* **2000**, *10*, 2755−2758.
(27) Cardillo, G.; Gentilucci, L.; Qasem, A. R.; Sgarzi, F.; Spampinato, S. Endomorphin-1 analogues containing beta-proline are mu-opioid receptor agonists and display enhanced enzymatic hydrolysis resistance. *J. Med. Chem.* **2002**, *45*, 2571−2578.
(28) Keresztes, A.; Szucs, M.; Borics, A.; Kover, K. E.; Forro, E.; Fulop, F.; Tomboly, C.; Peter, A.; Pahi, A.; Fabian, G.; Muranyi, M.; Toth, G. New endomorphin analogues containing alicyclic beta-amino acids: influence on bioactive conformation and pharmacological profile. *J. Med. Chem.* **2008**, *51*, 4270−4279.
(29) Staniszewska, R.; Fichna, J.; Gach, K.; Toth, G.; Poels, J.; Vanden Broeck, J.; Janecka, A. Synthesis and biological activity of endomorphin-2 analogs incorporating piperidine-2-, 3- or 4-carboxylic acids instead of proline in position 2. *Chem. Biol. Drug Des.* **2008**, *72*, 91−94.
(30) Zhao, D. P.; Yang, D. X.; Wang, Y. J.; Wang, Y.; Mao, L. J.; Wang, R. Enantioselective Mannich reaction of a highly reactive Horner−Wadsworth−Emmons reagent with imines catalyzed by a bifunctional thiourea. *Chem. Sci.* **2011**, *2*, 1918−1921.
(31) Rang, H. P. Stimulant actions of volatile anaesthetics on smooth muscle. *Br. J. Pharmacol. Chemother.* **1964**, *22*, 356−365.
(32) Hughes, J.; Kosterlitz, H. W.; Leslie, F. M. Effect of morphine on adrenergic transmission in the mouse vas deferens. Assessment of agonist and antogonist potencies of narcotic analgesics. *Br. J. Pharmacol.* **1975**, *53*, 371−381.

(33) Mallareddy, J. R.; Borics, A.; Keresztes, A.; Kover, K. E.; Tourwe, D.; Toth, G. Design, synthesis, pharmacological evaluation, and structure−activity study of novel endomorphin analogues with multiple structural modifications. *J. Med. Chem.* **2011**, *54*, 1462−1472.
(34) Li, T.; Fujita, Y.; Tsuda, Y.; Miyazaki, A.; Ambo, A.; Sasaki, Y.; Jinsmaa, Y.; Bryant, S. D.; Lazarus, L. H.; Okada, Y. Development of potent mu-opioid receptor ligands using unique tyrosine analogues of endomorphin-2. *J. Med. Chem.* **2005**, *48*, 586−592.
(35) Liu, H. M.; Liu, X. F.; Yao, J. L.; Wang, C. L.; Yu, Y.; Wang, R. Utilization of combined chemical modifications to enhance the blood−brain barrier permeability and pharmacological activity of endomorphin-1. *J. Pharmacol. Exp. Ther.* **2006**, *319*, 308−316.
(36) Sasaki, Y.; Sasaki, A.; Niizuma, H.; Goto, H.; Ambo, A. Endomorphin 2 analogues containing Dmp residue as an aromatic amino acid surrogate with high mu-opioid receptor affinity and selectivity. *Bioorg. Med. Chem.* **2003**, *11*, 675−678.
(37) Yabaluri, N.; Medzihradsky, F. Down-regulation of mu-opioid receptor by full but not partial agonists is independent of G protein coupling. *Mol. Pharmacol.* **1997**, *52*, 896−902.
(38) Koda, Y.; Del Borgo, M.; Wessling, S. T.; Lazarus, L. H.; Okada, Y.; Toth, I.; Blanchfield, J. T. Synthesis and in vitro evaluation of a library of modified endomorphin 1 peptides. *Bioorg. Med. Chem.* **2008**, *16*, 6286−6296.
(39) Sim, L. J.; Liu, Q.; Childers, S. R.; Selley, D. E. Endomorphin-stimulated [^{35}S]GTPgammaS binding in rat brain: evidence for partial agonist activity at mu-opioid receptors. *J. Neurochem.* **1998**, *70*, 1567−1576.
(40) Hosohata, K.; Burkey, T. H.; Alfaro-Lopez, J.; Varga, E.; Hruby, V. J.; Roeske, W. R.; Yamamura, H. I. Endomorphin-1 and endomorphin-2 are partial agonists at the human mu-opioid receptor. *Eur. J. Pharmacol.* **1998**, *346*, 111−114.
(41) Belcheva, M. M.; Szucs, M.; Wang, D.; Sadee, W.; Coscia, C. J. mu-Opioid receptor-mediated ERK activation involves calmodulin-dependent epidermal growth factor receptor transactivation. *J. Biol. Chem.* **2001**, *276*, 33847−33853.
(42) Morou, E.; Georgoussi, Z. Expression of the third intracellular loop of the delta-opioid receptor inhibits signaling by opioid receptors and other G protein-coupled receptors. *J. Pharmacol. Exp. Ther.* **2005**, *315*, 1368−1379.
(43) Sanchez-Blazquez, P.; Rodriguez-Diaz, M.; DeAntonio, I.; Garzon, J. Endomorphin-1 and endomorphin-2 show differences in their activation of mu opioid receptor-regulated G proteins in supraspinal antinociception in mice. *J. Pharmacol. Exp. Ther.* **1999**, *291*, 12−18.
(44) Liu, X.; Kai, M.; Jin, L.; Wang, R. Molecular modeling studies to predict the possible binding modes of endomorphin analogs in mu opioid receptor. *Bioorg. Med. Chem. Lett.* **2009**, *19*, 5387−5391.
(45) Befort, K.; Tabbara, L.; Bausch, S.; Chavkin, C.; Evans, C.; Kieffer, B. The conserved aspartate residue in the third putative transmembrane domain of the delta-opioid receptor is not the anionic counterpart for cationic opiate binding but is a constituent of the receptor binding site. *Mol. Pharmacol.* **1996**, *49*, 216−223.
(46) Chen, C.; Yin, J.; Riel, J. K.; DesJarlais, R. L.; Raveglia, L. F.; Zhu, J.; Liu-Chen, L. Y. Determination of the amino acid residue involved in [^{3}H]beta-funaltrexamine covalent binding in the cloned rat mu-opioid receptor. *J. Biol. Chem.* **1996**, *271*, 21422−21429.
(47) Li, J. G.; Chen, C.; Yin, J.; Rice, K.; Zhang, Y.; Matecka, D.; de Riel, J. K.; DesJarlais, R. L.; Liu-Chen, L. Y. ASP147 in the third transmembrane helix of the rat mu opioid receptor forms ion-pairing with morphine and naltrexone. *Life Sci.* **1999**, *65*, 175−185.
(48) Mansour, A.; Taylor, L. P.; Fine, J. L.; Thompson, R. C.; Hoversten, M. T.; Mosberg, H. I.; Watson, S. J.; Akil, H. Key residues defining the mu-opioid receptor binding pocket: a site-directed mutagenesis study. *J. Neurochem.* **1997**, *68*, 344−353.
(49) Mosberg, H. I.; Fowler, C. B. Development and validation of opioid ligand−receptor interaction models: the structural basis of mu vs delta selectivity. *J. Pept. Res.* **2002**, *60*, 329−335.
(50) Surratt, C. K.; Johnson, P. S.; Moriwaki, A.; Seidleck, B. K.; Blaschak, C. J.; Wang, J. B.; Uhl, G. R. -mu opiate receptor. Charged transmembrane domain amino acids are critical for agonist recognition and intrinsic activity. *J. Biol. Chem.* **1994**, *269*, 20548−20553.
(51) Shahrestanifar, M.; Wang, W. W.; Howells, R. D. Studies on inhibition of mu and delta opioid receptor binding by dithiothreitol and *N*-ethylmaleimide. His223 is critical for mu opioid receptor binding and inactivation by *N*-ethylmaleimide. *J. Biol. Chem.* **1996**, *271*, 5505−5512.
(52) Manglik, A.; Kruse, A. C.; Kobilka, T. S.; Thian, F. S.; Mathiesen, J. M.; Sunahara, R. K.; Pardo, L.; Weis, W. I.; Kobilka, B. K.; Granier, S. Crystal structure of the micro-opioid receptor bound to a morphinan antagonist. *Nature* **2012**, *485*, 321−326.
(53) Wang, C. L.; Yao, J. L.; Yu, Y.; Shao, X.; Cui, Y.; Liu, H. M.; Lai, L. H.; Wang, R. Structure−activity study of endomorphin-2 analogs with C-terminal modifications by NMR spectroscopy and molecular modeling. *Bioorg. Med. Chem.* **2008**, *16*, 6415−6422.
(54) In, Y.; Minoura, K.; Tomoo, K.; Sasaki, Y.; Lazarus, L. H.; Okada, Y.; Ishida, T. Structural function of C-terminal amidation of endomorphin. Conformational comparison of mu-selective endomorphin-2 with its C-terminal free acid, studied by ^{1}H-NMR spectroscopy, molecular calculation, and X-ray crystallography. *FEBS J.* **2005**, *272*, 5079−5097.
(55) Toth, G.; Kramer, T. H.; Knapp, R.; Lui, G.; Davis, P.; Burks, T. F.; Yamamura, H. I.; Hruby, V. J. [D-Pen^{2},D-Pen^{5}]Enkephalin analogues with increased affinity and selectivity for delta opioid receptors. *J. Med. Chem.* **1990**, *33*, 249−253.
(56) Hruby, V. J.; Bartosz-Bechowski, H.; Davis, P.; Slaninova, J.; Zalewska, T.; Stropova, D.; Porreca, F.; Yamamura, H. I. Cyclic enkephalin analogues with exceptional potency and selectivity for delta-opioid receptors. *J. Med. Chem.* **1997**, *40*, 3957−3962.
(57) Fichna, J.; do-Rego, J. C.; Costentin, J.; Chung, N. N.; Schiller, P. W.; Kosson, P.; Janecka, A. Opioid receptor binding and in vivo antinociceptive activity of position 3-substituted morphiceptin analogs. *Biochem. Biophys. Res. Commun.* **2004**, *320*, 531−536.
(58) Kruszynski, R.; Fichna, J.; do-Rego, J. C.; Chung, N. N.; Schiller, P. W.; Kosson, P.; Costentin, J.; Janecka, A. Novel endomorphin-2 analogs with mu-opioid receptor antagonist activity. *J. Pept. Res.* **2005**, *66*, 125−131.
(59) Fichna, J.; do-Rego, J. C.; Chung, N. N.; Lemieux, C.; Schiller, P. W.; Poels, J.; Broeck, J. V.; Costentin, J.; Janecka, A. Synthesis and characterization of potent and selective mu-opioid receptor antagonists, [Dmt^{1},D-2-Nal^{4}]endomorphin-1 (Antanal-1) and [Dmt^{1},D-2-Nal^{4}]endomorphin-2 (antanal-2). *J. Med. Chem.* **2007**, *50*, 512−520.
(60) Dai, Y.; Iwata, K.; Fukuoka, T.; Kondo, E.; Tokunaga, A.; Yamanaka, H.; Tachibana, T.; Liu, Y.; Noguchi, K. Phosphorylation of extracellular signal-regulated kinase in primary afferent neurons by noxious stimuli and its involvement in peripheral sensitization. *J. Neurosci.* **2002**, *22*, 7737−7745.
(61) Megaritis, G.; Merkouris, M.; Georgoussi, Z. Functional domains of delta- and mu-opioid receptors responsible for adenylyl cyclase inhibition. *Recept. Channels* **2000**, *7*, 199−212.
(62) Pinyot, A.; Nikolovski, Z.; Bosch, J.; Segura, J.; Gutierrez-Gallego, R. On the use of cells or membranes for receptor binding: growth hormone secretagogues. *Anal. Biochem.* **2010**, *399*, 174−181.
(63) Mitch, C. H.; Quimby, S. J.; Diaz, N.; Pedregal, C.; de la Torre, M. G.; Jimenez, A.; Shi, Q.; Canada, E. J.; Kahl, S. D.; Statnick, M. A.; McKinzie, D. L.; Benesh, D. R.; Rash, K. S.; Barth, V. N. Discovery of aminobenzyloxyarylamides as kappa opioid receptor selective antagonists: application to preclinical development of a kappa opioid receptor antagonist receptor occupancy tracer. *J. Med. Chem.* **2011**, *54*, 8000−8012.
(64) Frandsen, E. K.; Krishna, G. A simple ultrasensitive method for the assay of cyclic AMP and cyclic GMP in tissues. *Life Sci.* **1976**, *18*, 529−541.
(65) Obermeier, H.; Wehmeyer, A.; Schulz, R. Expression of mu-, delta- and kappa-opioid receptors in baculovirus-infected insect cells. *Eur. J. Pharmacol.* **1996**, *318*, 161−166.
(66) Wei, Q.; Zhou, D. H.; Shen, Q. X.; Chen, J.; Chen, L. W.; Wang, T. L.; Pei, G.; Chi, Z. Q. Human mu-opioid receptor overexpressed in

Sf9 insect cells functionally coupled to endogenous Gi/o proteins. *Cell Res.* **2000**, *10*, 93−102.
(67) Gusovsky, F. Measurement of Second Messengers in Signal Transduction: cAMP and Inositol Phosphates. In *Current Protocols in Neuroscience*; Wiley: New York, 2001; Chapter 7, Unit 7.12.
(68) Korzh, A.; Keren, O.; Gafni, M.; Bar-Josef, H.; Sarne, Y. Modulation of extracellular signal-regulated kinase (ERK) by opioid and cannabinoid receptors that are expressed in the same cell. *Brain Res.* **2008**, *1189*, 23−32.
(69) Belcheva, M. M.; Clark, A. L.; Haas, P. D.; Serna, J. S.; Hahn, J. W.; Kiss, A.; Coscia, C. J. Mu and kappa opioid receptors activate ERK/MAPK via different protein kinase C isoforms and secondary messengers in astrocytes. *J. Biol. Chem.* **2005**, *280*, 27662−27669.
(70) Schmidt, H.; Schulz, S.; Klutzny, M.; Koch, T.; Handel, M.; Hollt, V. Involvement of mitogen-activated protein kinase in agonist-induced phosphorylation of the mu-opioid receptor in HEK 293 cells. *J. Neurochem.* **2000**, *74*, 414−22.
(71) Gillespie, T. J.; Konings, P. N.; Merrill, B. J.; Davis, T. P. A specific enzyme assay for aminopeptidase M in rat brain. *Life Sci.* **1992**, *51*, 2097−2106.
(72) Liu, X.; Kai, M.; Jin, L.; Wang, R. Computational study of the heterodimerization between mu and delta receptors. *J. Comput.-Aided Mol. Des.* **2009**, *23*, 321−332.
(73) Berendsen, H. J.; Vanderspoel, D.; Vandrunen, R. GROMACS: a message-passing parallel molecular dynamics implementation. *Comput. Phys. Commun.* **1995**, *91*, 43−56.
(74) Vanbuuren, A. R.; Marrink, S. J.; Berendsen, H. J. C. A molecular dynamics study of the decane/water interface. *J. Phys. Chem.* **1993**, *97*, 9206−9212.
(75) Darden, T.; York, D.; Pedersen, L. Particle mesh Ewald: an *N*-log(*N*) method for Ewald sums in large system. *J. Chem. Phys.* **1993**, *98*, 10089−10092.
(76) Hess, B.; Bekker, H.; Berendsen, H. J. C.; Fraaije, J. LINCS: a linear constraint solver for molecular simulations. *J. Comput. Chem.* **1997**, *18*, 1463−1472.
(77) Berendsen, H. J. C.; Postma, J. P. M.; Vangunsteren, W. F.; Dinola, A.; Haak, J. R. Molecular dynamics with coupling to an external bath. *J. Chem. Phys.* **1984**, *81*, 3684−3690.
(78) Morris, G. M.; Goodsell, D. S.; Halliday, R. S.; Huey, R.; Hart, W. E.; Belew, R. K.; Olson, A. J. Automated docking using a Lamarckian genetic algorithm and an empirical binding free energy function. *J. Comput. Chem.* **1998**, *19*, 1639−1662.
(79) Yu, Y.; Shao, X.; Cui, Y.; Liu, H. M.; Wang, C. L.; Fan, Y. Z.; Liu, J.; Dong, S. L.; Cui, Y. X.; Wang, R. Structure−activity study on the spatial arrangement of the third aromatic ring of endomorphins 1 and 2 using an atypical constrained C terminus. *ChemMedChem* **2007**, *2*, 309−317.
(80) Hetenyi, C.; van der Spoel, D. Efficient docking of peptides to proteins without prior knowledge of the binding site. *Protein Sci.* **2002**, *11*, 1729−1737.
(81) Hetenyi, C.; van der Spoel, D. Blind docking of drug-sized compounds to proteins with up to a thousand residues. *FEBS Lett.* **2006**, *580*, 1447−1450.
(82) Hetenyi, C.; Paragi, G.; Maran, U.; Timar, Z.; Karelson, M.; Penke, B. Combination of a modified scoring function with two-dimensional descriptors for calculation of binding affinities of bulky, flexible ligands to proteins. *J. Am. Chem. Soc.* **2006**, *128*, 1233−1239.
(83) Schuttelkopf, A. W.; van Aalten, D. M. PRODRG: a tool for high-throughput crystallography of protein−ligand complexes. *Acta Crystallogr., Sect. D: Biol. Crystallogr.* **2004**, *60*, 1355−1363.
(84) DeLano, W. L. *The PyMOL Molecular Graphics System*; DeLano Scientific: Palo Alto, CA, U.S., 2002.